IEEE Access
Multidisciplinary ⋮ Rapid Review ⋮ Open Access Journal

Received 7 March 2024, accepted 24 March 2024, date of publication 27 March 2024, date of current version 4 April 2024.

Digital Object Identifier 10.1109/ACCESS.2024.3382569

RESEARCH ARTICLE

A Distributed Architecture of Parallel Buck-Boost Converters and Cascaded Control of DC Microgrids-Real Time Implementation

MOHAMED A. MESBAH[1], KHAIRY SAYED[2], (Member, IEEE), ADEL AHMED[3], MAHMOUD AREF[3], MAHMOUD A. GAAFAR[4], (Member, IEEE), MAHMOUD A. MOSSA[5], MISHARI METAB ALMALKI[6], AND THAMER A. H. ALGHAMDI[6,7]

[1]Faculty of Technology and Education, Sohag University, Sohag 1673040, Egypt
[2]Electrical Engineering Department, College of Engineering, Sohag University, Sohag 1646130, Egypt
[3]Department of Electrical Engineering, Assiut University, Assiut 71516, Egypt
[4]Aswan Power Electronics Applications Research Center (APEARC), Faculty of Engineering, Aswan University, Aswan 81542, Egypt
[5]Electrical Engineering Department, Faculty of Engineering, Minia University, Minia 61111, Egypt
[6]Department of Electrical Engineering, Faculty of Engineering, Al-Baha University, Alaqiq 65779-7738, Saudi Arabia
[7]Wolfson Centre for Magnetics, School of Engineering, Cardiff University, CF24 3AA Cardiff, U.K.

Corresponding authors: Mahmoud A. Mossa (mahmoud_a_mossa@mu.edu.eg) and Thamer A. H. Alghamdi (Alghamdit1@cardiff.ac.uk)

ABSTRACT To enhance the stability and reliability of the system, the converters' parallel operation can be cascaded to address the constraints posed by the substantial integration of renewable resources. Buck-boost DC-DC converters are often controlled via a cascaded control approach to allow parallel operation. The converter's output current and its voltage will be controlled by nested loop control. This study proposes adaptive droop control parameters that are updated and verified online using the principal current sharing loops to minimize the fluctuation in load current sharing. When the converters in the microgrid are paralleled, load sharing will be accomplished using the droop control approach in addition to nested proportional-integral-based voltage and current control loops. To restore the correct voltage across the DC microgrid, an outer addition voltage secondary loop will be used, rectifying any voltage disparities caused by the droop management strategy. Several common load resistances and input voltage variations are used to test the suggested method. Using a linearized model, this work assesses the stability and performance of the proposed method. It then confirms the findings with an adequate model created in MATLAB/SIMULINK, Real-Time Simulation Fundamentals, and hardware-based experiments.

INDEX TERMS Adaptive droop control, distribution generator, DC microgrid, droop control, distributed energy resources, discontinuous conduction mode.

I. INTRODUCTION

Microgrids MGs are becoming more and more popular as a means of resolving energy and environmental problems because of their ability to effectively integrate distributed generators that are interfaced with converters, including fuel cells, batteries, wind, solar, and solar power. Many applications have been found for power electronics converters. DC-based distribution systems are being used widely due to the growth of distributed energy resources, electronics loads, electric vehicles, and energy storage devices in microgrid systems [1]. Due to its ability to effectively incorporate distributed generation and eliminate complicated frequency and reactive power regulation concerns, as well as the AC/DC and DC/AC conversion phases, DC microgrids have recently attracted increased interest [2]. DC-DC converters are among

The associate editor coordinating the review of this manuscript and approving it for publication was Zhilei Yao.

the most efficient power electronic devices for regulating DC voltage and enhancing the performance of renewable energy systems. An essential component that significantly affects the power systems' overall performance is the choice of DC-DC converter, in a buck-boost converter, however, the output voltage is controlled in relation to the input voltage both less and greater [3].

When compared with more modern buck-boost converter topologies, the traditional buck-boost converter could not perform as well [4]. The advantages of the traditional buck-boost converter include its easy construction, cost-effectiveness, and ability to achieve both voltage step-up and down, as well as features that are typical of more modern buck-boost converters [5]. In recent years, traditional buck-boost converters have been the subject of extensive research and are used in a variety of systems, including PV production, DC power supply, and motor drive systems. Therefore, to investigate the suggested techniques for DC microgrid control [6], the traditional buck-boost topology is used in this work.

In contrast to alternative systems of cascading converters, the output voltage as well as the voltage and current sharing of each module are controlled by the dynamical effects of the buck-boost converter [7]. In [8], the goals of the dynamic droop control are to meet the DC microgrid's needs for voltage management and current sharing. It suggests configuring large-signal PI controllers in a way that can maintain optimum power sharing even when power stage parameters change and realize near-time optimal transient improvement in single converters. To manage the output voltage of the buck-boost converter, a sliding mode controller has been constructed [9]. This controller only uses one voltage control loop and is not capable of controlling the inductor's current. Additionally, the switching frequency is changeable, making filter design challenging and potentially causing unwanted current harmonics [10]. For controlling the outer voltage loop, a linear controller is utilized, while the inner current loop is controlled by a hysteresis controller based on sliding mode control [11]. The sliding mode control technique for independent microgrid voltage and frequency regulation has been implemented in real time employing a digital signal processor controller. However, because of the oscillations on a switching surface, this control approach exhibits considerable ripple. Sliding mode control-based control techniques have been used extensively in industry in recent decades because of their remarkable durability [12], [13]. In subsequent studies, the impacts of communication on the stability and performance of the microgrid will be examined, along with distributed control of a suggested predictive control by proximal processes [14].

In order to incorporate the sources into the utility grid and EV applications, there were more parts and they were all part of a time-sharing plan [15]. The issues with conventional droop control are addressed by hierarchical or centralized control techniques, which leverage communication links between the converters. For the centralized controller, local DC-bus voltage cannot be restored if the communication link or the central control unit malfunctions. As a result, the hybrid control method a blend of hierarchical, centralized, decentralized, and droop is used for both concurrent power-sharing and regulation of DC-bus voltage [16]. For the system to become more reliable overall, planning and protection must be well coordinated. Two primary reasons for this necessity are the erratic nature of renewable energy supply and the dynamic load profiles [17]. Figure 1 shows a DC microgrid consisting of DC-DC converters in the parallel buck-boost converter configuration.

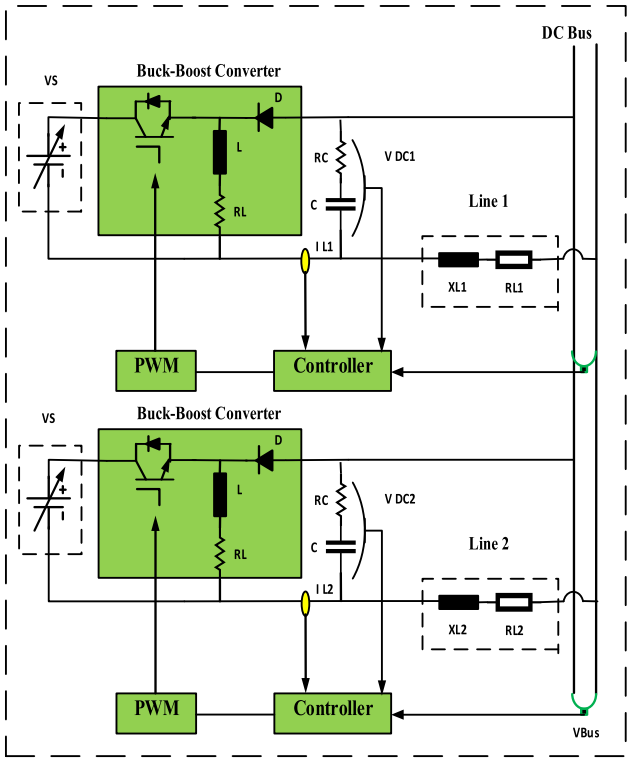

FIGURE 1. Power sources structure of buck-boost converter parallel interface.

The fundamental goal of DC microgrid control is to regulate the voltage output of the current sharing among the converters by using a method that is both acceptable and efficient [18]. The effectiveness of traditional droop is significantly impacted by line impedance. Both linear and non-linear modes can be employed with the droop control technique [19], [20]. It was decided to use the non-linear droop mechanism since line impedance negatively affects the linear droop mechanism. It has been noted that the non-linear properties of droop control cause a delay in the trade-off between voltage regulation and current sharing [21], [22]. Because the converters communicate more effectively and transfer data more quickly, the distributed control approach can provide adaptive droop control at the secondary and primary control levels [23]. The droop coefficient can be softly adjusted under different loading scenarios thanks to the adaptive droop gain technique [24], [25]. At the secondary

level, regulators of voltage and current are used to provide terms for voltage and impedance adjustment. The primary current-sharing loops were used for modifying the parameters of droop control and checking them online to reduce the variance of current sharing in the load [26], [27]. To remove the bus voltage fluctuations in the DC microgrids, the buck-boost converter uses a second loop in addition to shifting the droop lines [28]. To make sure that every converter in DC microgrids shares load appropriately, The virtual resistances in the previous section are continuously updated by using the main loop [29], [30].

This paper presents a unique adaptive control system for the buck-boost converter that provides correct current sharing and enhances the corresponding droop gains with increasing load, contingent on the loading state and variable input. The creative and innovative adaptive droop controller does this by transferring the droop lines to minimize fluctuation of the DC-bus voltage of the DC microgrid and by checking and changing the droop parameters online, utilizing the main current-sharing loops, to lessen the variation of current sharing in load. A computed time vector and a step change in the input voltage and load, from 10 to 5 and 3.33 ohm, respectively, are utilized to evaluate the proposed approach with variable input, load resistances, and a range of input voltages. MATLAB/SIMULINK steps the model. Establishing a connection, the OPAL-RT OP4510 Real-Time Simulation workflow starts with instantaneous testing and simulation.

The method and outcomes also demonstrate how the suggested improved buck-boost converter adaptive droop control strategy:

- Preserves the DC microgrid's power balance under significant disturbances with effectiveness.
- Enhances energy sharing and precisely controls DC-DC bus voltages under a variety of operating conditions.
- Improves the DC-DC microgrid's capacity for stability and its ability to react quickly to disturbances.
- Enhances modularity, scalability, adaptability, and dependability of DC-DC microgrids.

II. MATERIALS AND METHODS

A. SYSTEM CONFIGURATION FOR THE BUCK-BOOST DC-DC CONVERTER

The DC microgrids seen in Figure 1 are made up of many parallel connection converters to share current between scattered sources at a common DC bus. The main objective of DC microgrid control is to achieve a reasonable and effective regulated output voltage for the converters' shared current. With changeable input voltage and load resistance as shown in Figure 2 (A), and fixed input voltage and changeable load resistance as shown in Figure 2 (B), the Buck-Boost converters configuration is shown in Figure 2. This research presents a novel adaptive control technique for the buck-boost converter that improves the equivalent droop gains.

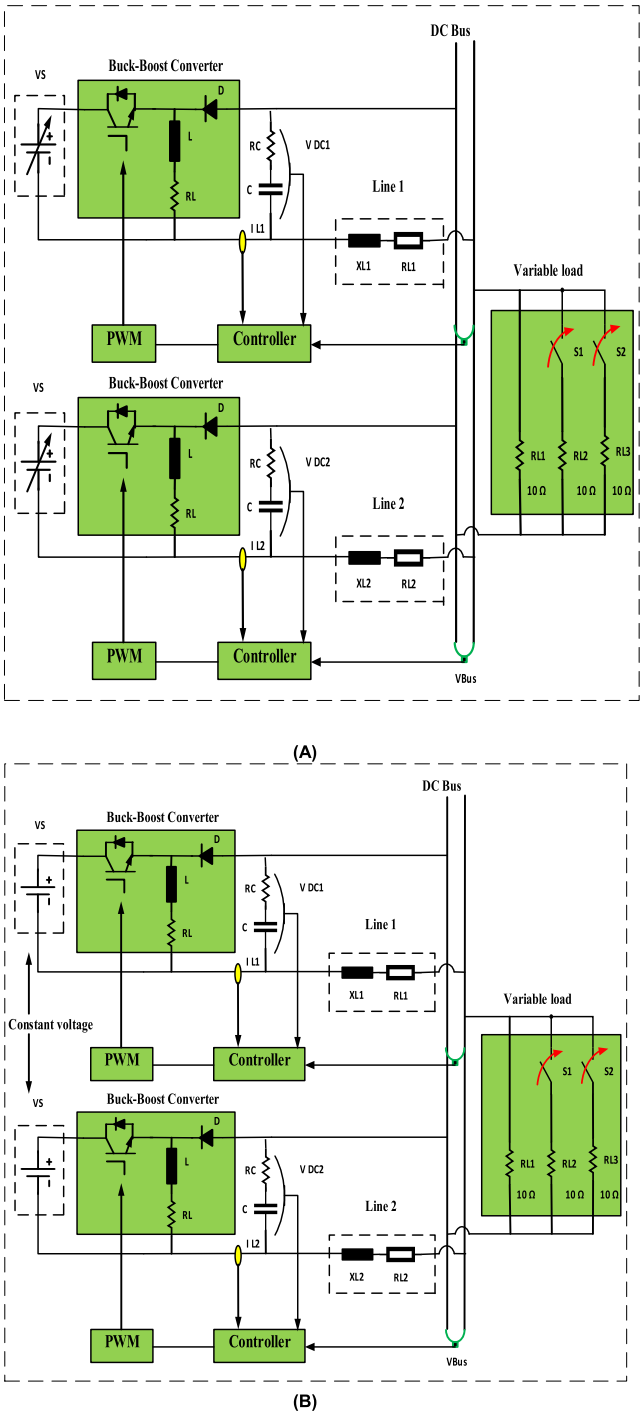

FIGURE 2. Configuration for buck-boost DC-DC converter with (A) Changeable input voltage and changeable load resistance and (B) Fixed input voltage and changeable load resistance.

B. STATE-SPACE FORMULAS

Assuming that every component is perfect, the circuit should have no internal resistance and energy-efficient components. By utilizing the average approach, the following may be determined:

1) BUCK CONVERTER

When the switch is closed

$$\begin{bmatrix}\dot{x}_1\\ \dot{x}_2\end{bmatrix}=\begin{bmatrix}0 & -\frac{1}{L}\\ \frac{1}{c} & -\frac{1}{Rc}\end{bmatrix}\begin{bmatrix}x_1\\ x_2\end{bmatrix}+\begin{bmatrix}\frac{1}{L}\\ 0\end{bmatrix}v_{in} \quad (1)$$

$$\dot{x}_1 = A_1x+B_1\mu \quad (2)$$

When the switch is open

$$\begin{bmatrix}\dot{x}_1\\ \dot{x}_2\end{bmatrix}=\begin{bmatrix}0 & -\frac{1}{L}\\ \frac{1}{c} & -\frac{1}{Rc}\end{bmatrix}\begin{bmatrix}x_1\\ x_2\end{bmatrix}+\begin{bmatrix}0\\ 0\end{bmatrix}v_{in} \quad (3)$$

$$\dot{x}_1 = A_2x+B_2\mu \quad (4)$$

The average model is obtained by taking the means of the state space matrices of the two distinct operating modes.

$$\begin{bmatrix}\dot{x}_1\\ \dot{x}_2\end{bmatrix}=\begin{bmatrix}0 & -\frac{1}{L}\\ \frac{1}{c} & -\frac{1}{Rc}\end{bmatrix}x+\begin{bmatrix}\frac{d}{L}\\ 0\end{bmatrix}v_{in} \quad (5)$$

where $\bar{A}$ and $\bar{B}$ as shown in equation 6 and 7.

$$\bar{A}=\begin{bmatrix}0 & -\frac{1}{L}\\ \frac{1}{c} & -\frac{1}{Rc}\end{bmatrix} \quad (6)$$

$$\bar{B}=\begin{bmatrix}\frac{d}{L}\\ 0\end{bmatrix} \quad (7)$$

where $\hat{I}_l(t)$, $\hat{I}_c(t)$, $\hat{I}_{in}(t)$, $\hat{d}$, $V_{in}(t)$and $\hat{v}_0(t)$minimal ac fluctuations surrounding the quiescent values of the input voltage, duty cycle, output voltage, inductor current, and capacitor current, correspondingly. The equivalent circuit buck converter as shown Figure 3, can be made simpler to produce the version that produces the necessary transfer functions.

$$\frac{Ld\hat{I}_l(t)}{dt} = D\hat{v}_{in}+\hat{d}v_{in}-\hat{v}_0(t) \quad (8)$$

$$\hat{I}_c(t) = \frac{cd\hat{v}_o(t)}{dt} = \hat{I}_l(t)-\frac{\hat{v}_o(t)}{R} \quad (9)$$

$$\hat{I}_{in}(t) = D\hat{I}_l(t)+\hat{d}I_l \quad (10)$$

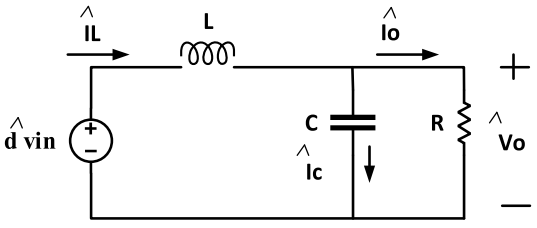

FIGURE 3. Simplified small signal equivalent circuit buck converter.

Obtained by applying the mathematical model formulas for linearized tiny signals, which are provided by Equations (8), (9) and (10).

$$\frac{\hat{I}_l(s)}{\hat{d}} = \frac{V_{in}(SCR+1)}{S^2CLR+SL+R} \quad (11)$$

$$\frac{\hat{v}_o(s)}{\hat{I}_l(s)} = \frac{R}{SCR+1} \quad (12)$$

The transfer functions of the duty cycle to the inductor current and the inductor current to the output voltage can be determined by converting the small signal mathematical model equations to the s-domain and utilizing the small signal equivalent circuit, which are provided by Equations (11) and (12).

2) BOOST CONVERTER

When the switch is closed

$$\begin{bmatrix}\dot{x}_1\\ \dot{x}_2\end{bmatrix}=\begin{bmatrix}0 & -\frac{1}{L}\\ 0 & -\frac{1}{Rc}\end{bmatrix}\begin{bmatrix}x_1\\ x_2\end{bmatrix}+\begin{bmatrix}\frac{1}{L}\\ 0\end{bmatrix}v_{in} \quad (13)$$

$$\dot{x}_1 = A_1x+B_1\mu \quad (14)$$

When the switch is open

$$\begin{bmatrix}\dot{x}_1\\ \dot{x}_2\end{bmatrix}=\begin{bmatrix}0 & -\frac{1}{L}\\ \frac{1}{c} & -\frac{1}{Rc}\end{bmatrix}\begin{bmatrix}x_1\\ x_2\end{bmatrix}+\begin{bmatrix}\frac{1}{L}\\ 0\end{bmatrix}v_{in} \quad (15)$$

$$\dot{x}_1 = A_2x+B_2\mu \quad (16)$$

The average model is obtained by taking the means of the state space matrices of the two distinct operating modes.

$$\begin{bmatrix}\dot{x}_1\\ \dot{x}_2\end{bmatrix}=\begin{bmatrix}0 & -\frac{(1-d)}{L}\\ \frac{(1-d)}{c} & -\frac{1}{Rc}\end{bmatrix}x+\begin{bmatrix}\frac{1}{L}\\ 0\end{bmatrix}v_{in} \quad (17)$$

where $\bar{A}$ and $\bar{B}$ as shown in equation 18 and 19.

$$\bar{A}=\begin{bmatrix}0 & -\frac{(1-d)}{L}\\ \frac{(1-d)}{c} & -\frac{1}{Rc}\end{bmatrix} \quad (18)$$

$$\bar{B}=\begin{bmatrix}\frac{1}{L}\\ 0\end{bmatrix} \quad (19)$$

The equivalent circuit boost converter as shown Figure 4, can be made simpler to produce the version that produces the necessary transfer functions. Where $\hat{I}_l(t)$, $\hat{I}_c(t)$, $\hat{I}_{in}(t)$, $\hat{d}$, $V_{in}(t)$ and $\hat{v}_0(t)$ minimal ac fluctuations surrounding the quiescent values of the input voltage, duty cycle, output voltage, inductor current, and capacitor current, correspondingly.

$$\frac{Ld\hat{I}_l(t)}{dt} = \hat{v}_{in}+D\hat{v}_0(t)+\hat{d}v_o \quad (20)$$

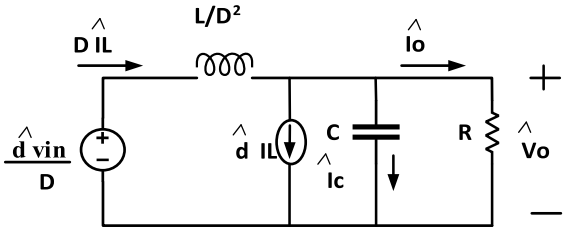

FIGURE 4. Simplified small signal equivalent circuit boost converter.

$$\hat{I}_c(t) = \frac{cd\hat{v}_o(t)}{dt} = -\frac{\hat{v}_o(t)}{R} + D\hat{I}_l(t) - \hat{d}I_l \tag{21}$$

$$\hat{I}_{in}(t) = \hat{I}_l(t) \tag{22}$$

By applying the mathematical model formulas for linearized tiny signals, which are provided by Equations (20), (21) and (22).

$$\frac{\hat{I}_l(s)}{\hat{d}} = \frac{SCRV_o + V_o + I_lRD}{S^2CLR + SL + RD^2} \tag{23}$$

$$\frac{\hat{v}_o(s)}{\hat{I}_l(s)} = \frac{DRV_o - SLRI_l}{SCRV_o + V_o + I_lRD} \tag{24}$$

By converting the small signal mathematical model equations to the s-domain and utilizing the small signal equivalent circuit, which are provided by Equations (23) and (24).

3) THE ADAPTIVE CONTROL TECHNIQUE

DC microgrid system. Achieving equal nominal voltages for the converter leads to the most accuracy in current sharing. The local control modifies each converter's nominal voltage to ensure precise current sharing error. Reduced current value sharing is found in converters with reduced maximum voltage deviation and nominal voltage. Therefore, the controller is configured to increase the nominal DC voltage based on the bus voltage deviation and the current load sharing. To do this, each converter's reference voltage is adjusted using a virtual resistance, R droop. R droop can be adjusted to control the power-sharing and reference voltage of any converter. Higher nominal voltage values are associated with converters with lesser voltage deviations. As the low voltage converter's nominal voltage approaches the second one, the current-sharing error decreases. In addition, the secondary loop reduces the voltage variation.

4) THE PRIMARY CONTROL LOOP

The primary loop's objective is to guarantee precise load sharing among all converters in DC microgrids. The proposed adaptive droop is elucidated using the droop diagram, as shown in Figure 5, which provides a flowchart sequence for the suggested approach. The *Rd*, values must be precisely adjusted to control the source converters and increase the bus voltage to guarantee that every converter generates an identical output voltage. Based on the bus voltage's maximum deviation from the DC microgrids, the suggested control must then distribute the load current nearly equally, which means that the converters' output voltages must be aligned.

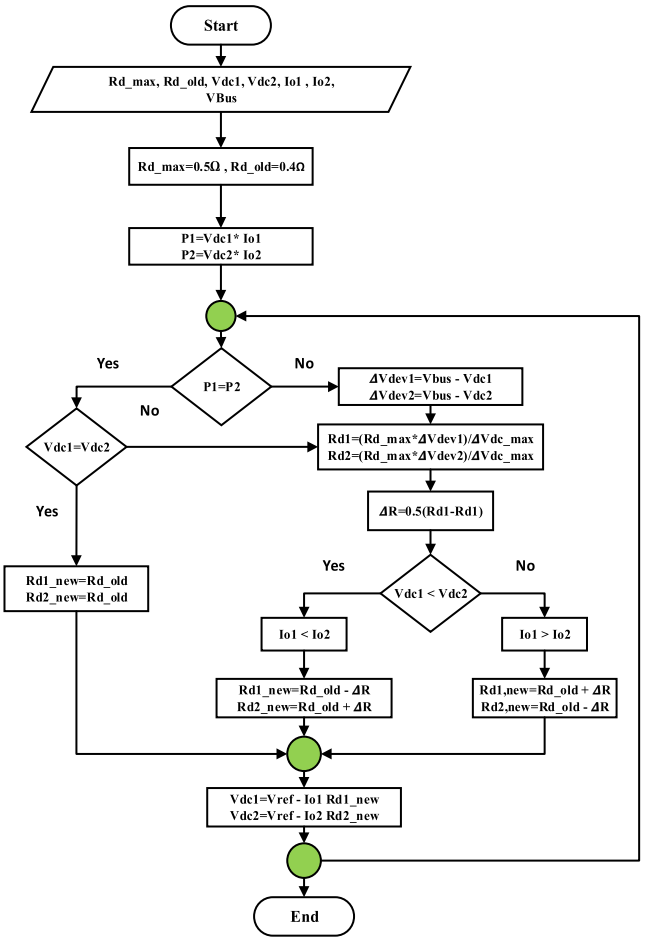

FIGURE 5. The suggested droop control method strategy's flowchart sequence.

1) Difference AT $V_{difference} = (V_{dc1} - V_{dc2})$ is positive value, $V_{O1} > V_{O2} > R_{d2} > R_{d1}$, $I_{O,2} < I_{O,1}$, the value for Rd droop is given as follows:

$$R_{d1,new} = \left(R_{d1,old} \pm \Delta R\right) \tag{25}$$

1) Difference AT $V_{difference} = (V_{dc1} - V_{dc2})$ is negative value, $V_{O1} < V_{O2} > R_{d1} > R_{d2}$, $I_{O,1} < I_{O,2}$, the value for Rd droop is given as follows:

$$R_{d1,new} = \left(R_{d1,old} \mp \Delta R\right) \tag{26}$$

1) Difference AT $V_{difference} = (V_{dc1} - V_{dc2})$ is zero value, the value for Rd droop is given as follows:

$$R_{d1,new} = \left(R_{di,old}\right) \tag{27}$$

5) THE SECONDARY CONTROL LOOP

In order to ensure that every converter in DC microgrids is properly distributing the load, the virtual resistance value from the previous section is continuously updated via the primary loop. The load influences the variance of the bus voltage, as does any malfunction in the current or voltage feedback. Figure 6 shows how the bus voltage variance from

TABLE 1. DC-DC buck-boots converter parameters in DC microgrids.

Parameters	Symbol	Values
Resistance of line-1	Rc1	0.1 Ω
Resistance of line-2	Rc2	0.2 Ω
Inductance of line-1	Lc1	0.2mH
Inductance of line-2	Lc2	0.4mH
Resistance of capacitor 1	r_1	0.03 Ω
Resistance of capacitor 2	r_1	0.03 Ω
Capacitor 1	C1	4000μF
Capacitor 2	C2	4000μF
Inductance 1	L1	0.1mH
Inductance 2	L2	0.1mH

TABLE 2. DC-DC buck-boots converter operating parameters in DC microgrids.

Operating Parameters	Symbol	Values
Input Voltage	V_{in}	60-90 V
Output Voltage	V_{out}	50-120 V
Maximum output current	I_{out}	15 A
Switching Frequency	F_{sw}	100 KHz
Operating Power	P_{out}	900 W
Current Converter #1 PI	K_P	0.002
Current Converter #1 PI	K_I	0.1
Voltage Converter #1 PI	K_P	0.01
Voltage Converter #1 PI	K_I	0.1
Voltage Restoration Converter #1 PI	K_P	4
Voltage Restoration Converter #1 PI	K_I	0.7
Current Converter #2 PI	K_P	0.002
Current Converter #2 PI	K_I	0.1
Voltage Converter #2 PI	K_P	0.03
Voltage Converter #2 PI	K_I	0.1
Voltage Restoration Converter #2 PI	K_P	5
Voltage Restoration Converter #2 PI	K_I	0.7

the DC microgrids is compensated for by using a second loop. Table 1 shows DC-DC Buck-Boots converter parameters, and table 2 shows the operating parameters in DC microgrids.

As shown in Figure 4, the secondary loop adjusted the voltage reference of the drooping line to manage and increase the bus voltage while maintaining the same current sharing for each converter in the microgrid. The PI controller will be used to compare the needed value, *VMG* with the measured bus voltage *VMG* to obtain the voltage deviation signal.

$$\Delta v_{mG} = K_{\rho i}\left(v_{MG,ref-}v_{MG}\right) + k_{i1}\int\left(v_{MG,ref-}v_{MG}\right)dt \quad (28)$$

The voltage deviation value ΔVMG shifts each converter to bring the bus voltage back to the necessary level. Updates

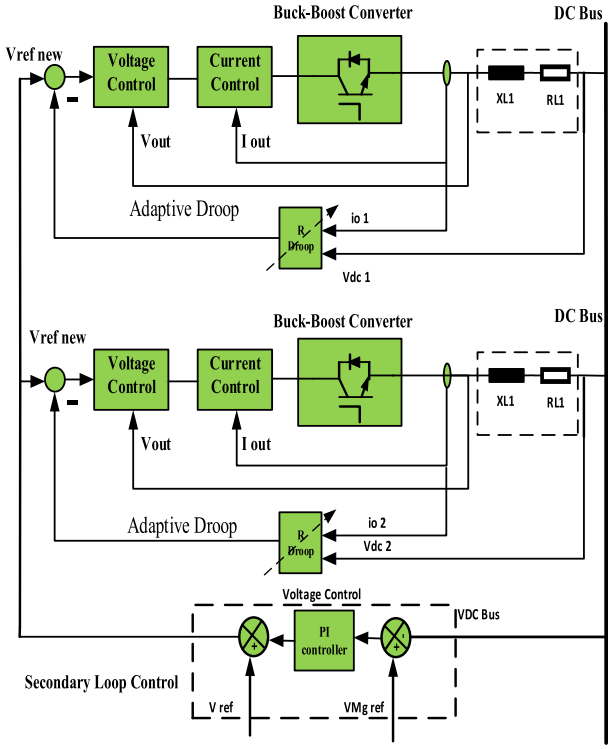

FIGURE 6. Adaptive control technique with a parallel buck-boost converter control scheme.

to the droop characteristic reference voltage look like this:

$$v_{dc1} = v_{dc}^{*} + \Delta v_{MG1} - i_{0,i} \times R_{d1} \quad (29)$$

$$v_{dc2} = v_{dc}^{*} + \Delta v_{MG2} - i_{0,i} \times R_{d2} \quad (30)$$

With the equation, For DC microgrids, bus voltage measurements can be computed rather than measured.

$$v_{MG} = v_{load} = v_{dci} - i_{0,i} \times (R_{d1} + R_{line2}) \quad (31)$$

The bus voltage variation is determined by the load and/or error in the current or voltage feedback. To counteract the bus voltage divergence from the DC microgrids, a second loop is employed, as illustrated in Figure 4. The restoration voltage is added to the output voltage $V_o$equation in the following way:

$$V_0 = V_{ref} + V_{res} - R_{droop} i_L \quad (32)$$

Measures of the performance of the suggested adaptive controller can therefore be greatly enhanced by Real-Time Simulation OPAL-RT OP4510 during its creation and evaluation when the suggested algorithm is assessed utilizing an Increasing trust in the power grid operator with changing input voltage and variable load resistance, as well as constant input voltage and variable load resistance. To verify the extent to which the suggested control system is operational, Figure 7 illustrates the presentation of voltage and current waveforms along with the performance of actual findings. When the load is varied in steps from 10 to 5 and 3.33 ohm when the input voltage is altered and constant input voltage and variable load resistance, MATLAB/SIMULINK step the model using a computed time vector. After determining the previous time

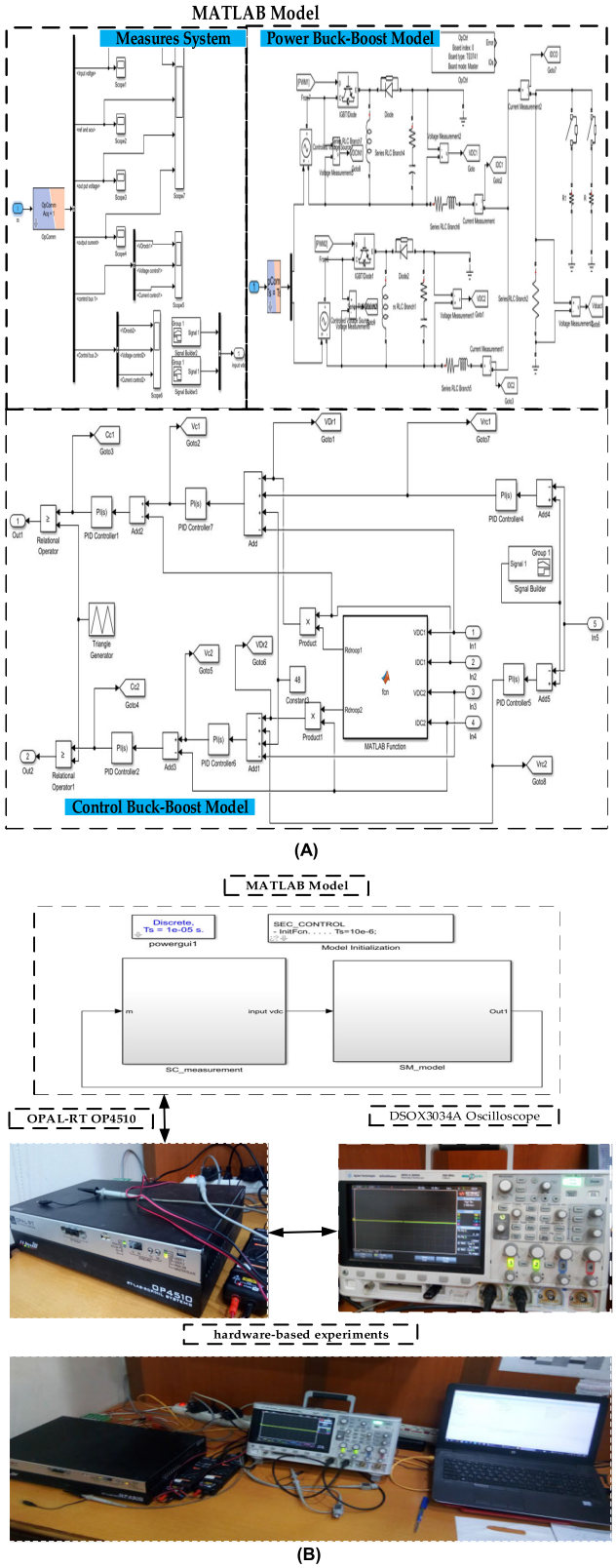

FIGURE 7. (A) Show simulation buck-boost model. (B) Configuration for real-time OPAL-RT OP4510.

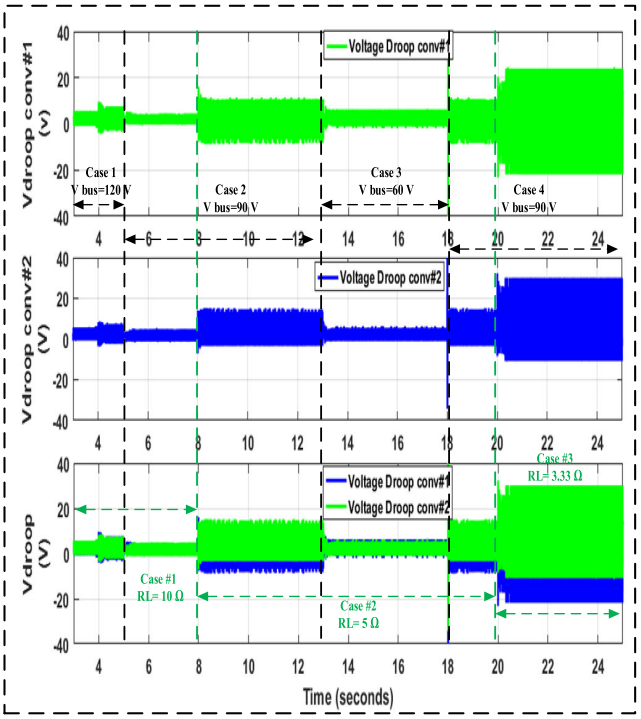

FIGURE 8. The transient response droop voltage for variable input voltage and variable load resistance MATLAB/SIMULINK from 10 Ω to 5 Ω and 3.33 Ω.

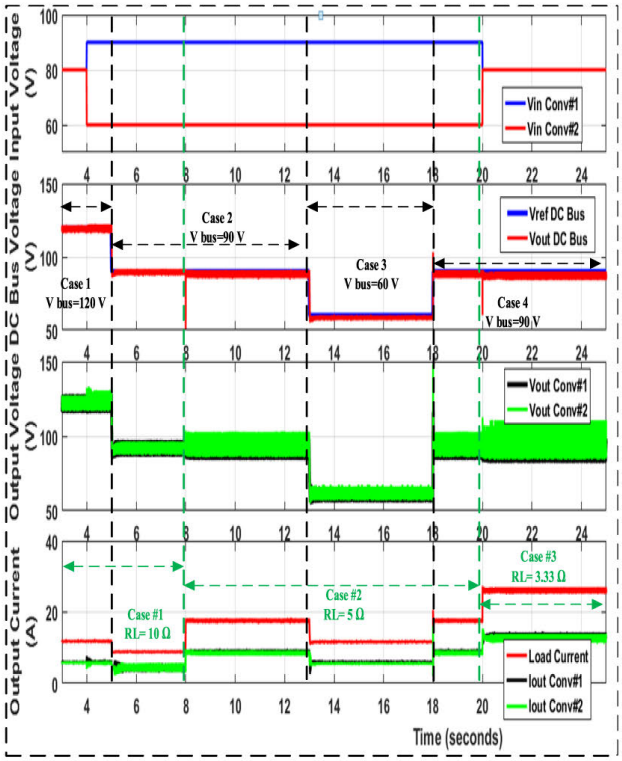

FIGURE 9. The transient response for variable input voltage and variable load resistance MATLAB/SIMULINK from 10 Ω to 5 Ω and 3.33 Ω.

value, Simulink quickly computes the outputs for the subsequent time value. This process is repeated until the stop time is reached. Regarding Instantaneous Simulation Real-time simulation and testing, connecting to the DSOX3034A

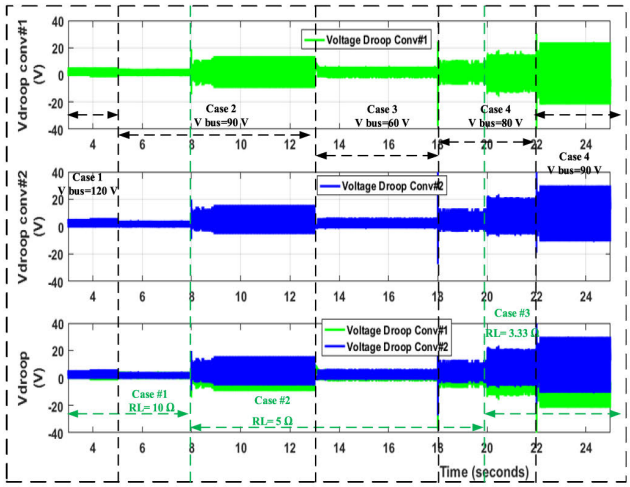

FIGURE 10. The transient response droop voltage for constant input voltage and variable load resistance MATLAB/SIMULINK from 10 Ω to 5 Ω and 3.33 Ω.

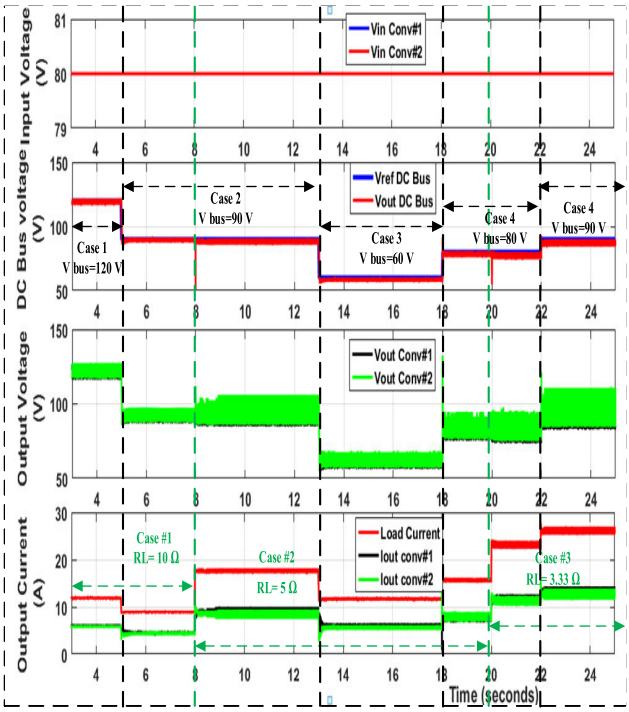

FIGURE 11. The transient response for constant input voltage and variable load resistance MATLAB/SIMULINK from 10 Ω to 5 Ω and 3.33 Ω.

Oscilloscope serial trigger and analysis, and segmented memory testing at any time are the first steps in the OPAL-RT OP4510 workflow.

III. RESULTS

This paper offers a practical examination apparatus for verifying the proposed algorithm control. For example, applications, such as the cascaded control method for parallel operation of buck-boost DC/DC converters, MATLAB/SIMULINK and Real-Time Simulation OPAL-RT

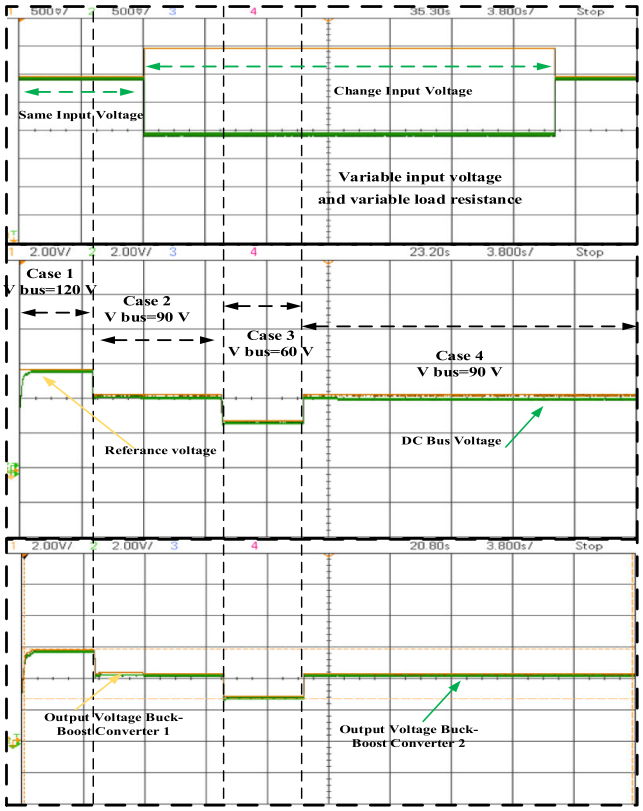

FIGURE 12. Variable input voltage and output bus voltage, and output voltage of two Buck-Boost converters at 10 Ω to 5 Ω and 3.33 Ω load variations.

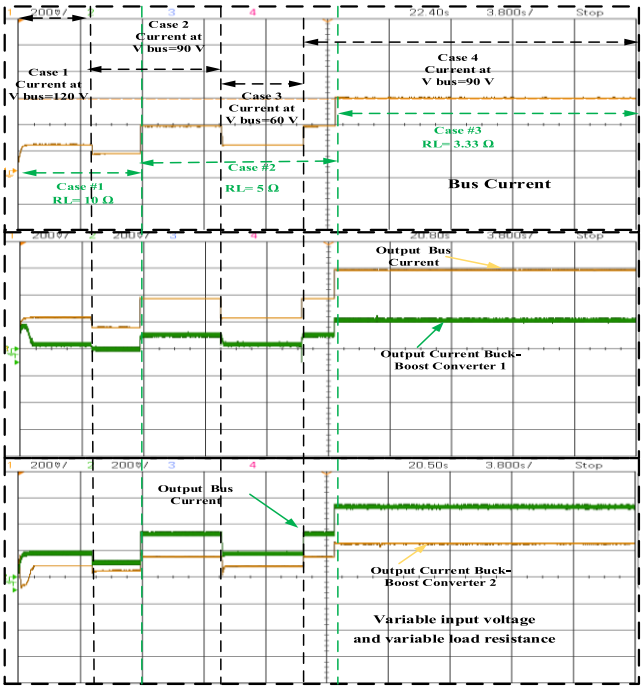

FIGURE 13. Output bus current, and output current of two buck-boost converters at 10 Ω to 5 Ω and 3.33 Ω load variations and input voltage changes.

OP4510 were used to simulate and analyze test procedures of the proposed control algorithm. Figure 8 shows the

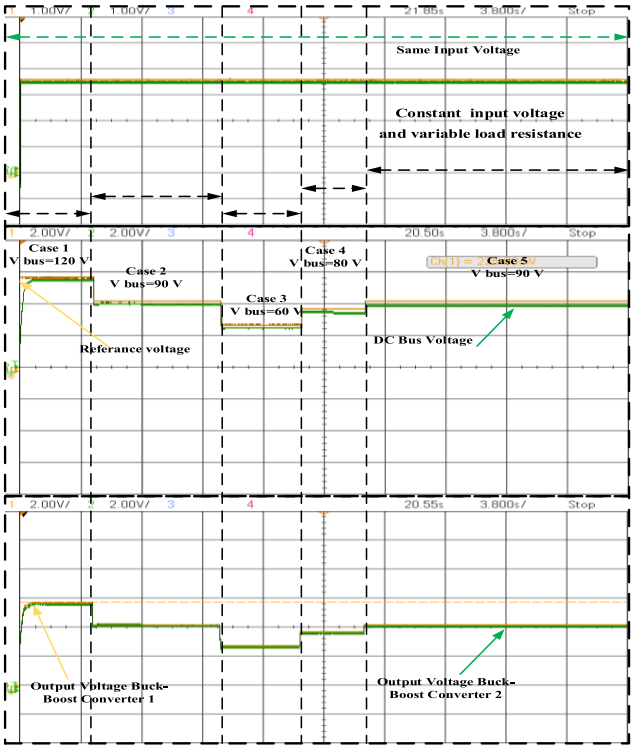

FIGURE 14. Both the constant input voltage and output bus voltage, and output voltage of two Buck-Boost converters at 10 Ω to 5 Ω and 3.33 Ω load variations.

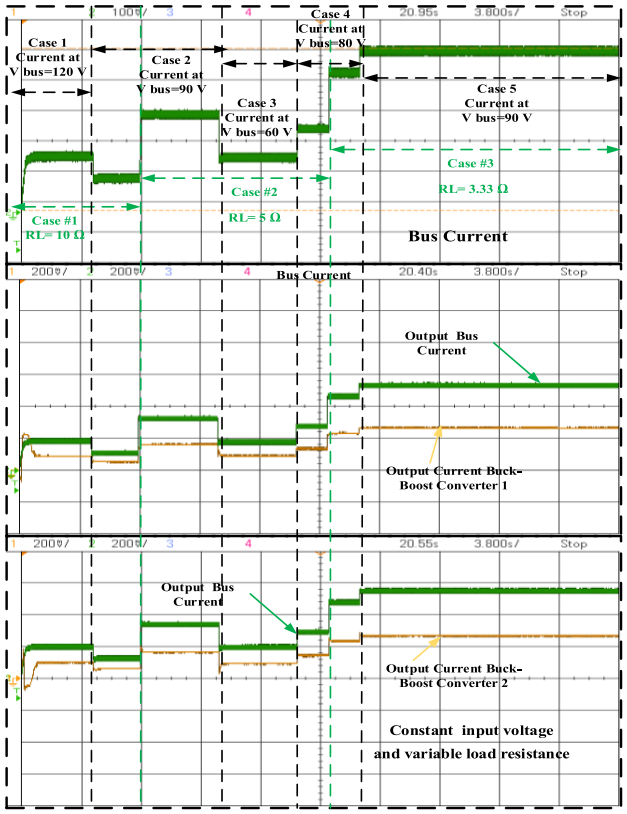

FIGURE 15. Output bus current, and output current of two Buck-Boost converters at 10 Ω to 5 Ω and 3.33 Ω load variations and constant input voltage.

transient response drop voltage for changeable input voltage and changeable load resistance MATLAB/SIMULINK from 10 Ω to 5 Ω and 3.33 Ω and Figure 9 shows the transient response for variable input voltage and variable load resistance MATLAB/SIMULINK from 10 Ω to 5 Ω and 3.33 Ω. In the results of the MATLAB program, there is some distortion in the voltage and current waves, but in the laboratory results there is no effect of the voltage and current waves, as the circuit was operated at switching frequency 100 k Hz. Figures 10 and 11 shows the transient response Droop Voltage and input voltage and variable load resistance for constant input voltage and variable load resistance MATLAB/SIMULINK from 10 Ω to 5 Ω and 3.33 Ω, compared with the result from Real-Time Simulation OPAL-RT OP4510 as shown figures 12, 13, 14 and 15.

IV. DISCUSSION

The suggested cascaded control method improves the performance of current sharing in droop control DC microgrids and removes bus voltage variation. Two loops are suggested: one improves current sharing, while the other keeps the bus voltage at its presumptive level. There are no measurements or communication linkages needed between the source converters when using the straightforward suggested control mechanism. Various operating situations are used to examine and assess the control methodology. The strength of the proposed technique is validated by considering the effect of the line impedance on the two Buck-Boost converters. The proposed controllers' experimental results agreed with the modelling results. Under various operational situations, the suggested technique performs better and is easier to execute. Table 3 shows the advantages and disadvantages of the

TABLE 3. Advantages and disadvantages of the control technique proposed.

Advantages	Disadvantages
• Secondary control layer handles the microgrid stability. • Distributed controllers can provide solutions for the entire system by exchanging information with one another. • Distributed control makes it possible for loads and resources to operate independently in a variety of situations. Distributed control thereby increases the system's reliability. • Good dynamic response. • Good voltage regulation. • Good current sharing due to direct current control.	• The system requires more sensors. • Sensitive current sharing with inadequate noise immunity.

control technique proposed, dynamic performance, current sharing accuracy and resolution capability.

V. CONCLUSION

This paper proposes a novel cascaded control method for the concurrent operation of buck-boost DC/DC converters. Adaptive droop control settings have been validated online and adjusted utilizing the major current sharing loops to reduce load current sharing fluctuations. The droop control method will be used to provide load sharing once the converters in the microgrid are paralleled. Furthermore, a voltage synchronization controller that can accommodate the requirements of a buck-boost converter as well as layered proportional-integral based voltage and current control loops will be constructed. The effectiveness and improved performance of the proposed control technique are confirmed and demonstrated with a hardware experimental setup that consists of two parallel buck-boost converters operating within a DC microgrid. To test the suggested approach, different input voltages and typical load resistances are employed. Furthermore, the same design process as the proposed cascaded voltage- and current-loop control method can be used to regulate the output voltage of a variety of DC-DC converters. As a result, the recommended control strategies must have a good reference value and flexibility. In the next study, we will investigate the applicability of the proposed control strategies for different kinds of DC-DC converters and DC microgrid management with complex DC-DC converter topologies. but the system requires more sensors, and Sensitive current sharing with inadequate noise immunity.

REFERENCES

[1] S. Sarangi, B. K. Sahu, and P. K. Rout, "A comprehensive review of distribution generation integrated DC microgrid protection: Issues, strategies, and future direction," *Int. J. Energy Res.*, vol. 45, no. 4, pp. 5006–5031, Mar. 2021, doi: 10.1002/er.6245.

[2] C. A. Soriano-Rangel, W. He, F. Mancilla-David, and R. Ortega, "Voltage regulation in buck–boost converters feeding an unknown constant power load: An adaptive passivity-based control," *IEEE Trans. Control Syst. Technol.*, vol. 29, no. 1, pp. 395–402, Jan. 2021, doi: 10.1109/TCST.2019.2959535.

[3] F. Mumtaz, N. Zaihar Yahaya, S. Tanzim Meraj, B. Singh, R. Kannan, and O. Ibrahim, "Review on non-isolated DC–DC converters and their control techniques for renewable energy applications," *Ain Shams Eng. J.*, vol. 12, no. 4, pp. 3747–3763, Dec. 2021, doi: 10.1016/j.asej.2021.03.022.

[4] S. Muchande and S. Thale, "Design and implementation of autonomous low voltage DC microgrid with hierarchical control," in *Proc. IEEE 1st Int. Conf. Smart Technol. Power, Energy Control (STPEC)*, Sep. 2020, pp. 1–6, doi: 10.1109/STPEC49749.2020.9297748.

[5] B. Zhu, S. Hu, G. Liu, Y. Huang, and X. She, "Low-voltage stress buck-boost converter with a high-voltage conversion gain," *IEEE Access*, vol. 8, pp. 95188–95196, 2020, doi: 10.1109/ACCESS.2020.2995889.

[6] T. Hashemi, R. Mahboobi Esfanjani, and H. Jafari Kaleybar, "Composite switched Lyapunov function-based control of DC–DC converters for renewable energy applications," *Electronics*, vol. 13, no. 1, p. 84, Dec. 2023.

[7] S. Kapat, "Small-signal analysis of parallelly connected buck converters and nonlinear droop control design for ultra-fast transient performance in DC microgrids," in *Proc. IEEE 1st Ind. Electron. Soc. Annu. On-Line Conf. (ONCON)*, Dec. 2022, pp. 1–6.

[8] M. Lv, P. Wang, Y. Wei, C. Wen, J. Li, P. Jia, and Q. Wei, "An input-series-output-parallel cascaded converter system applied to DC microgrids," *Symmetry*, vol. 15, no. 6, p. 1174, May 2023, doi: 10.3390/sym15061174.

[9] M. K. Kavitha and A. Kavitha, "Nonlinear analysis of hysteretic modulation-based sliding mode controlled quadratic Buck–Boost converter," *J. Circuits, Syst. Comput.*, vol. 28, no. 02, Feb. 2019, Art. no. 1950025, doi: 10.1142/s0218126619500257.

[10] B.-R. Lin and M.-Y. Liu, "Parallel full-bridge converter for low voltage DC microgrid applications," in *Proc. 13th IEEE Conf. Ind. Electron. Appl. (ICIEA)*, May 2018, pp. 1050–1055, doi: 10.1109/ICIEA.2018.8397866.

[11] C. Yfoulis, S. Papadopoulou, and S. Voutetakis, "Robust linear control of boost and buck-boost DC–DC converters in micro-grids with constant power loads," *Energies*, vol. 13, no. 18, p. 4829, Sep. 2020, doi: 10.3390/en13184829.

[12] U. K. Kalla, B. Singh, S. S. Murthy, C. Jain, and K. Kant, "Adaptive sliding mode control of standalone single-phase microgrid using hydro, wind, and solar PV array-based generation," *IEEE Trans. Smart Grid*, vol. 9, no. 6, pp. 6806–6814, Nov. 2018, doi: 10.1109/TSG.2017.2723845.

[13] A. Marahatta, Y. Rajbhandari, A. Shrestha, S. Phuyal, A. Thapa, and P. Korba, "Model predictive control of DC/DC boost converter with reinforcement learning," *Heliyon*, vol. 8, no. 11, Nov. 2022, Art. no. e11416, doi: 10.1016/j.heliyon.2022.e11416.

[14] D. Murillo-Yarce, S. Riffo, C. Restrepo, C. González-Castaño, and A. Garcés, "Model predictive control for stabilization of DC microgrids in island mode operation," *Mathematics*, vol. 10, no. 18, p. 3384, Sep. 2022, doi: 10.3390/math10183384.

[15] M. Dhananjaya, M. Vellingiri, Z. M. Alaas, M. Rawa, M. Jagabar Sathik, D. Almakhles, and D. Potnuru, "New multi-source DC–DC boost converter and its generalized structure with experimental validation," *Ain Shams Eng. J.*, vol. 14, no. 10, Oct. 2023, Art. no. 102173, doi: 10.1016/j.asej.2023.102173.

[16] M. S. Alam, F. S. Al-Ismail, S. M. Rahman, M. Shafiullah, and M. A. Hossain, "Planning and protection of DC microgrid: A critical review on recent developments," *Eng. Sci. Technol., Int. J.*, vol. 41, May 2023, Art. no. 101404, doi: 10.1016/j.jestch.2023.101404.

[17] W. He, M. M. Namazi, H. R. Koofigar, M. A. Amirian, and J. M. Guerrero, "Voltage regulation of buck converter with constant power load: An adaptive power shaping control," *Control Eng. Pract.*, vol. 115, Oct. 2021, Art. no. 104891, doi: 10.1016/j.conengprac.2021.104891.

[18] M. Baranwal, A. Askarian, S. Salapaka, and M. Salapaka, "A distributed architecture for robust and optimal control of DC microgrids," *IEEE Trans. Ind. Electron.*, vol. 66, no. 4, pp. 3082–3092, Apr. 2019, doi: 10.1109/TIE.2018.2840506.

[19] M. Srinivasan and A. Kwasinski, "Control analysis of parallel DC–DC converters in a DC microgrid with constant power loads," *Int. J. Electr. Power Energy Syst.*, vol. 122, Nov. 2020, Art. no. 106207, doi: 10.1016/j.ijepes.2020.106207.

[20] D. Zammit, C. S. Staines, M. Apap, and A. Micallef, "Control of buck and boost converters for stand-alone DC microgrids," in *Proc. 8th Int. Symp. Energy*, Aberdeen, Scotland, U.K., Aug. 2018, no. August, pp. 6–9.

[21] J. Kreiss, M. Bodson, R. Delpoux, J.-Y. Gauthier, J.-F. Trégouët, and X. Lin-Shi, "Optimal control allocation for the parallel interconnection of buck converters," *Control Eng. Pract.*, vol. 109, Apr. 2021, Art. no. 104727, doi: 10.1016/j.conengprac.2021.104727.

[22] S. Ahmed, S. A. R. Kashif, N. U. Ain, A. Rasool, M. S. Shahid, S. Padmanaban, E. Ozsoy, and M. A. Saqib, "Mitigation of complex non-linear dynamic effects in multiple output cascaded DC–DC converters," *IEEE Access*, vol. 9, pp. 54602–54612, 2021, doi: 10.1109/ACCESS.2021.3071198.

[23] Z. Cheng, Z. Li, S. Li, J. Gao, J. Si, H. S. Das, and W. Dong, "A novel cascaded control to improve stability and inertia of parallel buck-boost converters in DC microgrid," *Int. J. Electr. Power Energy Syst.*, vol. 119, Jul. 2020, Art. no. 105950, doi: 10.1016/j.ijepes.2020.105950.

[24] F. G. Nimitti and A. M. S. S. Andrade, "Bidirectional converter based on boost/buck DC–DC converter for microgrids energy storage systems interface," *Int. J. Circuit Theory Appl.*, vol. 50, no. 12, pp. 4376–4394, Dec. 2022, doi: 10.1002/cta.3403.

[25] Y. Qin, Y. Yang, S. Li, Y. Huang, S.-C. Tan, and S. Y. Hui, "A high-efficiency DC/DC converter for high-voltage-gain, high-current applications," *IEEE J. Emerg. Sel. Topics Power Electron.*, vol. 8, no. 3, pp. 2812–2823, Sep. 2020, doi: 10.1109/JESTPE.2019.2908416.

[26] M. A. Mosa and A. A. Ali, "Energy management system of low voltage DC microgrid using mixed-integer nonlinear programing and a global optimization technique," *Electric Power Syst. Res.*, vol. 192, Mar. 2021, Art. no. 106971, doi: 10.1016/j.epsr.2020.106971.

[27] S. Dahale, A. Das, Naran. M. Pindoriya, and S. Rajendran, "An overview of DC–DC converter topologies and controls in DC microgrid," in *Proc. 7th Int. Conf. Power Syst. (ICPS)*, Dec. 2017, pp. 410–415, doi: 10.1109/ICPES.2017.8387329.

[28] H. M. Maheri, P. C. Heris, Z. Saadatizadeh, E. Babaei, and D. Vinnikov, "A new coupled-inductor-based buck/boost DC/DC converter with soft switching for DC microgrid applications," in *Proc. IEEE 15th Int. Conf. Compat., Power Electron. Power Eng. (CPE-POWERENG)*, Jul. 2021, pp. 1–6, doi: 10.1109/CPE-POWERENG50821.2021.9501195.

[29] A. Ingle, A. B. Shyam, S. R. Sahoo, and S. Anand, "Quality-index based distributed secondary controller for a low-voltage DC microgrid," *IEEE Trans. Ind. Electron.*, vol. 65, no. 9, pp. 7004–7014, Sep. 2018, doi: 10.1109/TIE.2018.2795524.

[30] Y. Zhang, X. Qu, M. Tang, R. Yao, and W. Chen, "Design of nonlinear droop control in DC microgrid for desired voltage regulation and current sharing accuracy," *IEEE J. Emerg. Sel. Topics Circuits Syst.*, vol. 11, no. 1, pp. 168–175, Mar. 2021, doi: 10.1109/JETCAS.2021.3049810.

MOHAMED A. MESBAH received the B.Sc. degree in power and electrical machine from the Department of Power and Electrical Machines, Faculty of Engineering–Helwan, Helwan University. He is currently pursuing the Ph.D. degree with the Faculty of Technology and Education, Sohag University. He was appointed as an Assistant Lecturer with the Faculty of Technology and Education, Sohag University.

KHAIRY SAYED (Member, IEEE) received the B.S. degree in electrical power and machines from Assiut University, Assiut, Egypt, in 1997, the master's degree from the Electrical Energy Saving Research Center, Graduate School of Electrical Engineering, Kyungnam University, Masan, South Korea, in 2007, and the Ph.D. degree from Assiut University, in 2013. He is currently an Associate Professor with the Department of Electrical Engineering, Sohag University, Egypt. His research interests include soft-switching dc–dc power converter topologies, high-frequency inverter applications, renewable energy-related power conditioners, and control schemes. He received the Best Student Paper Award from the 57th Annual Conference of the International Appliances Technical Conference IATC2006 held at Crowne Plaza, Chicago, IL, USA, March 27–29, and Sohag University Encouragement Awards in the field of engineering science, from 2016 to 2017.

ADEL AHMED received the B.Sc. and M.Sc. degrees in electrical engineering from Assiut University, Egypt, in 1987 and 1993, respectively, and the D.Eng. degree from the Institute of Theoretical Electrical Engineering, Technical University of Hamburg-Harburg, Germany, in 2001. He is currently a Professor with the Department of Electrical Engineering, Faculty of Engineering, Assiut University. His research interests include high voltage engineering, electrostatic applications in industry, power system analysis, renewable energy-related power conditioners, and control schemes.

MAHMOUD AREF was born in Sohag, Egypt, in 1984. He received the B.Sc. and M.Sc. degrees in electrical engineering from Assiut University, Egypt, in 2006 and 2012, respectively, and the Ph.D. degree from the Department of Automated Electrical Systems, Ural Power Engineering Institute, Ural Federal University, Russia, in 2020. He is currently an Assistant Professor with the Department of Electrical Engineering, Assiut University. His research interest includes the stability and reliability of renewable sources connected to electrical power systems.

MAHMOUD A. GAAFAR (Member, IEEE) received the B.Sc. and M.Sc. degrees in electrical engineering from Aswan University, Aswan, Egypt, in 2004 and 2010, respectively, and the Ph.D. degree in electrical and electronics engineering from Kyushu University, Fukuoka, Japan, in 2017. In 2017, he joined the Aswan Power Electronics Applications Research Center (APEARC), Aswan University. He is currently an Assistant Professor with the Department of Electrical Engineering, Faculty of Engineering, Aswan University. He has been involved in several projects related to power electronics applications. His current research interests include the design and control of power electronics converters for photovoltaic, motor drives, and battery-based systems. He is a member of the IEEE Power Electronics Society. He was a recipient of the Baek-Hyun Award from Korean Institute of Power Electronics, in 2018, for his academic contribution to the field of power electronics.

MAHMOUD A. MOSSA received the bachelor's and master's degrees in electrical engineering from the Faculty of Engineering, Minia University, Egypt, in 2008 and 2013, respectively, and the Ph.D. degree in electrical engineering, in April 2018. Since January 2010, he has been an Assistant Lecturer with the Electrical Engineering Department, Minia University. In November 2014, he joined the Electric Drives Laboratory (EDLAB), University of Padova, Italy, for the Ph.D. research activities. Since May 2018, he has been an Assistant Professor with the Electrical Engineering Department, Minia University, where he is currently an Associate Professor. He occupied a postdoctoral fellow position with the Department of Industrial Engineering, University of Padova, for six months. His research interests include renewable energy systems, power management, optimization, electric machine drives, power electronics, and load frequency control.

MISHARI METAB ALMALKI was born in Taif, Saudi Arabia, in November 1986. He received the B.Sc. degree from King Abdulaziz University (KAU), Saudi Arabia, in 2009, and the M.Sc. and Ph.D. degrees from Southern Illinois University, Carbondale, IL, USA, in 2013 and 2018, respectively. Since 2018, he has been an Assistant Professor of electrical engineering with Al Baha University, Al Aqiq, Saudi Arabia. His main research interests include power systems, power quality, power drives, smart grids, power distribution and protection, the integration of renewables, and AI applications in electrical power engineering.

THAMER A. H. ALGHAMDI received the B.Sc. degree from Al-Baha University, Saudi Arabia, in 2012, the M.Sc. degree from Northumbria University, U.K., in 2016, and the Ph.D. degree from Cardiff University, Cardiff, U.K., in 2023. He was a Power Distribution Engineer at Saudi Electricity Company (SEC), until 2013. From 2016 to 2018, he was a Lecturer Assistant with Al-Baha University, where he is currently an Assistant Professor of electrical power engineering with the Department of Electrical Engineering. His main research interests include power systems, power quality, the integration of renewables, and AI applications in electrical power engineering.